Use of a drone equipped with microthermal sensors to estimate the quality of the atmosphere for astronomical observation

José Antonio Quesada-Moreno[1], Emilio Martínez-Ibarra[1] and José Luis Ortiz[2]

[1]*Departamento de Análisis Geográfico Regional y Geografía Física, Universidad de Granada, Granada, Spain*

[2]*Instituto de Astrofísica de Andalucía, CSIC, Granada, Spain*

Introduction

Atmospheric turbulence severely disturbs the quality of the images taken through an astronomical optical telescope. As astronomy has developed, various different procedures have been applied to analyse the atmospheric potential of a particular place for astronomical observation purposes. These have ranged from subjective techniques, based on the expert opinion of an astronomer, to more recent technical and quantitative procedures. Subjective techniques based on visual observations were used until the beginning of the 20th century. In 1923, the American astronomer, Francis Pease, used an eyepiece in the focus (optics of the telescope) to observe the quality of an astronomical image, according to the appearance of the Moon, the planets and certain bright stars.

The quantitative techniques can be classified as direct or indirect. The former study the quality of the astronomical image (hereafter referred to as 'seeing'), while the latter infer this quality through atmospheric turbulence. Seeing is what is 'seen' either through a telescope or with the naked eye. If the atmospheric turbulence increases (so changing its refractive index) in a field crossed by light rays, the rays are randomly diffracted in different directions with respect to their true position, so affecting the quality of the image received even in a medium-power telescope.

The direct techniques are normally based on (1) short exposure photography (e.g. Lyot, 1945); (2) Polar Star Trails, using a fixed camera focused on the Pole Star (e.g. Walker, 1971; Birkle *et al.*, 1976); (3) the Differential Image Motion Monitor (DIMM), capable of measuring the intensity of the turbulence and inferring the quality of the image in an astronomical sense. Different versions of the DIMM can be found in Giovanelli *et al.* (2001), Tokovinin *et al.* (2003), Sánchez *et al.* (2007), McHught *et al.* (2008) and Fossat (2011); (4) SCIDAR (Scintillation Detection and Ranging) proposed by Vernin and Roddier (1973) and used by Vernin and Muñoz-Tuñón (1992) or the G-SCIDAR (Generalised Scintillation Detection and Ranging) (e.g. Egner and Masciadri, 2007); (5) SNODARS (Surface Layer Non-Doppler Acoustic Radar) (e.g. Bonner *et al.*, 2010) and (6) SLODARS (Slope Detection And Ranging), described by Wilson *et al.* (2004) as a tool for analysing seeing (i.e. the quality of an image in the astronomical sense). It uses masks on the telescope and double stars to determine the atmospheric turbulence profile, via triangulation.

For their part, the indirect techniques study vertical thermal profiles using microthermal sensors (e.g. Coulman *et al.*, 1986; Ulich and Davison, 1985; Ando *et al.*, 1989), and others such as thermal microvariations seen from satellites (Cavazzani *et al.*, 2012) or laser emitter-receiver techniques on the ground (Cavazzani *et al.*, 2014). The Obukhov-Kolmogorov theory of turbulence provides a link between the structure of the atmospheric thermal field and the optical properties of the atmosphere (Barletti *et al.*, 1977). For further information, the physical relationships between atmospheric turbulence and seeing quality have been reviewed in detail by Roddier (1981) and Coulman *et al.* (1986).

The term 'microthermal sensor' is normally used to refer to a device that measures the thermal differences (up to precision of thousandths of Kelvin) between two sensors, situated a certain distance, normally one metre, apart. At specified intervals, these sensors take slightly different measurements at the same horizontal level. From the differential measurements of the thermocouple, we obtained a microthermal RMS (root mean square). This is a useful base for the study of atmospheric turbulence and image quality in an astronomical sense. Various different authors have measured the RMS using thermocouples installed on balloon platforms (e.g. Bufton, 1975; Agabi *et al.*, 2006; McHught *et al.*, 2008; Fossat, 2011) or meteorological towers (Hartley *et al.*, 1981; Dhananjay, 2014). They all attempt to identify the optimum atmospheric properties and hence the turbulence index. As a rule, this is done by taking microthermal measurements in differential form between two sensors located 1m apart in the horizontal plane. The RMS is associated with a C_T^2 (Structure Coefficient of Temperature) parameter expressed in degC. The C_T^2 can be measured directly, using high-frequency response temperature sensors (microthermal sensors) located 1m apart, from the following expression:

$$C_{T^2} = \frac{\sigma^2_{(RMS)}}{r^{2/3}}, \qquad (1)$$

where $\sigma^2_{(RMS)}$ is the variance of the RMS or thermal noise, and r is the horizontal distance between the microthermal sensors (1m).

In this way, C_T^2 is a measure of the thermal turbulence in a given r.

In this research, we assess the possibilities of installing microthermal sensors on drones, so as to study atmospheric turbulence from an astronomical perspective. We begin by describing the sources and methodology, placing special emphasis on a possible new application for drones as a mobile medium for the study of the 'Planetary Boundary Layer' (PBL) and the surface or 'Ground Layer' (GL) and its influence on the conditions for astronomical observation. Later, we will set out the results obtained at different geographical locations representative of astronomical observation in the southeast of the Iberian Peninsula. The last section covers the discussion and main conclusions of this study.

Study area

In this study, we attempt to validate the use of drones for studying atmospheric

turbulence for astronomical observation purposes. To this end, we carried out nocturnal microthermal profiles in two mountainous areas in the southeast of the Iberian Peninsula in Andalusia (Figure 1), referred to here as Study Areas 1 and 2. Study Area 1 is the Hispanic Astronomy Centre (Centro Astronómico Hispano) situated at the top of Calar Alto, a mountain peak at 2168m asl (37°12′N and 2°33′W), in the Sierra of Los Filabres in the province of Almeria. Study Area 2 is situated at two sites in the Sierra de la Sagra in the northeast of the province of Granada, namely Pico Montilla, at 1800m asl (37°59′N and 2°34′W) and the astronomical observatory of La Sagra, at 1530m (37°58′N and 2°34′W) (Figure 1).

Due to the possible climatic influences on astronomical observation, it is important to make clear, as regards the local conditions of the sampling or study points, that measurements were taken at three quite different types of locations: (i) on a high plateau, as at Calar Alto (Figure 2); (ii) on a saddle between two mountains, as at the astronomical observatory of La Sagra (Figure 3) and (iii) on a nearby isolated peak, called Pico Montilla (Figure 4).

Sources and methodology

Our study is based on the use of microthermal measurements as a means of obtaining indirect measurements of seeing, according to the procedure proposed by Dhananjay (2014). The first step was to select the microthermal sensors and convert the resistance temperature detector (RTD) data into degrees Celsius. We decided to use PT 1000 microthermal sensors (RS PRO2), which are very stable and have time constants of around 0.1s. They have platinum RTD with tolerances specified in IEC 60751:2008. They comply with the international standard, presenting a coefficient of variation in the order of 3.85ΩK^{-1}, so enabling them to detect thermal variations, once translated into temperatures, of <0.003 degC (Table 1).

The procedure for converting the data into degrees Celsius was conducted indoors. We carried out 21 simultaneous measurements in which the differences in the voltage of the PT 1000 sensors were compared with the differences in temperature between two sensors of a digital thermometer for a thermal range of about 6 degC. The following should be considered in order to understand the process: (1) both PT 1000 sensors were used (PT1 and PT2); (2) The digital thermometer was an Auriol Item IAN 315731 with two sensors (d1 and d2). This thermometer has a resolution translated to its digital readout of 0.1 degC. It should be noted that although these thermometers have a typical response time of a few seconds, they are perfectly suitable for this purpose since the temperature was varied very slowly during the calibration process to adapt the data acquisition times to the inertia of the digital thermometer; (3) A controlled heat source using ~30W resistive was located inside a wooden box ('hot pole'). One PT 1000 sensor was placed inside the box together with the internal sensor of the digital thermometer. The other two sensors measured temperatures with no external heat source ('the cold pole') and were situated outside the box at a distance of one metre from the 'hot pole' and (4) An amplifier (CJMCU333) coupled to the PT 1000 probe resistors and a TTGO (esp-32) analogue–digital converter were used to display the output voltage values of the sensors in a PC. The data were transmitted to the PC via a LORA-type radio frequency transmitter.

The voltage reading from the PT 1000 amplifier output was converted to temperature in degC for the best regression model (R^2 of 0.9908) as follows:

$$y = 3.0069x + 0.272 \quad (2)$$

where x is the voltage measured at the amplifier output of the PT 1000 pair resistors and y is the differential between the temperatures measured by the digital thermometers (Figure 5). In this way, a variation of 1V is equivalent to approximately 3 degC. This is in line with the electrical specifications of the PT 1000 for which the

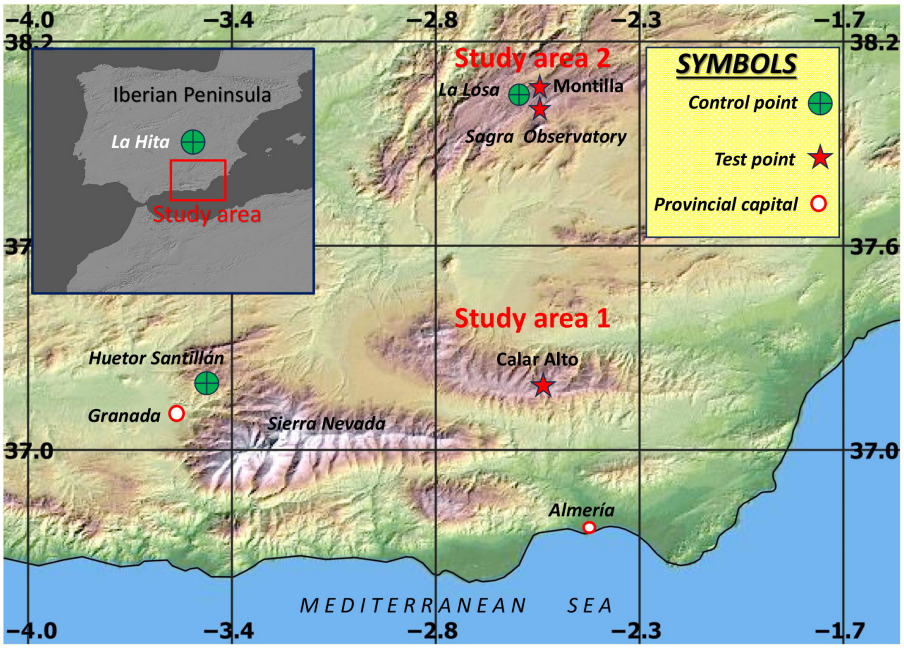

Figure 1. Study area indicating the sampling or study points.

Figure 2. Calar Alto observatory (early 1980s).

Figure 3. La Sagra observatory.

Figure 4. The Pico Montilla station near the peak of La Sagra (in the background).

variation in the coefficient of resistance is around $3.85\Omega K^{-1}$.

We then selected the drone for transporting the sensors. After a series of flights with the sensors, we decided to use the JRC Bugs 3 drone. This is a commercial drone, with a mass of 0.5kg. It has a flight time of about 20 min (although this varies according to the payload and the state of the atmosphere), and a maximum payload of about 250g. It is capable of reaching an altitude of 120–150m above the ground.

The drone was fitted with a 5m-long vertical wire to avoid the turbulence produced by the rotor blades (longer length did not improve RMS during control flights). A 1m-long horizontal rod was tied to the bottom of the wire and the microthermal sensors were installed at each end of the rod. The preamplification electronics, the analogue–digital converter and the radio transmitter (in our case a LORAN transmitter) were installed in the centre of the rod. A laptop was used as a receiver and for storage of the data (Figure 6).

The next stage was to test the technique for obtaining microthermal profiles with drones equipped with microthermal sensors in three places: in La Hita, 670m (39°34′N and 3°11′W) in the province of Toledo, where we made 4 RMS profiles; in Huetor Santillán, 1120m, (37°14′N and 3°31′W) in the province of Granada, where we made 7 RMS profiles (Figure 7) and in Puerto de la Losa, 1750m (38°0′N and 2°35′W) in the province of Granada, where we made 2 RMS profiles. In this way, we verified the viability of the procedure applied to obtain the RMS. In line with the recommendations of Bufton (1975), the flights were made at night, so avoiding the effects of solar irradiance on the sensors.

The next step was to select the places at which to make the profiles between 0 and 150m above the ground. We selected places that were representative of the southeast of the Iberian Peninsula in two study areas: (1) Area 1, the Hispanic Astronomy Centre of Andalusia situated on Calar Alto. Here we carried out 20 RMS profiles and (2) Area 2, two places in the NE of the province of Granada, that is, the astronomical observatory of La Sagra where we conducted 40 RMS profiles and Pico Montilla, where we conducted 18 RMS profiles.

Once we had obtained the thermal profiles, we then calculated the C_T^2.

It should be noted that when a plane wave of light with a uniform amplitude propagates through a non-refractively uniform medium, such as the Earth's atmosphere, it undergoes a measurable fluctuation in its amplitude and phase. When this plane wave is brought within the focus of a telescope, the displayed image of a stellar point undergoes variations in intensity, sharpness and position. These variations are generally referred to as 'scintillation', 'image blurring' and 'image motion' in that order. The long-exposure image size θ, or FWHM (Full Width at Half Maximum of the stellar profiles in a detector), is a measure of the combined effect of these variations. It is widely used in astronomy (hence our interest in calculating it here), and it is related to the force of thermal turbulence (C_T^2). This is why we considered C_T^2 in our calculation of FWHM, which we use as a measure of the quality of the image in an astronomical sense.

The FWHM is a measure of the average variability of the refractive index of light in the atmosphere. It is measured in arcsecs and represents the full width at half maximum of the stellar images in a detector. We studied the first 150m of height at each point analysed. To this end, we considered the astronomical applications of turbulence theory, which were originally systematised by VanZandt *et al.* (1978, 1981) and then referred to and extended, among others by Vernin and Muñoz-Tuñon (1992), Tokovinin (2002), Tokovinin *et al.* (2003), McHught *et al.* (2008) and Zago (2010). In our case, we moved directly from the C_T^2 to the FWHM of the seeing disc for the average environmental conditions on a mountain (pressure 770hPa, temperature 10°C). The FWHM was calculated by simplifying the intermediate steps and from the following expression:

Table 1

Characteristics of our microthermal measurement system.

Parameter	*PT 1000 RS PRO 2 sensor (standard: EC 751)*	*CJMCU333 (amplifier)*	*TTGO (esp-32) A/D &T/R*
Frequency			2.4 GZ
Resistance	1000Ω		
Measuring temperature range	[– 50, 500] °C	[– 40, +125] °C	
TCR/TCI (at 27°C)	3.85Ω degC^{-1}		
Gain used	1×	30×	1×
Temperature resolution	<0.003 degC		
Time constant of the sensor	<0.1s (water)		
Sampling rate	–	–	10 Hz
ADC voltage levels	3.3V	3.7V	3.7V
ADC steps	–	–	2048 steps
Digitization step size	–		0.001V
Drifting	Negligible	<25μV	–
Self-heating	<0.5 degCmW^{-1}	–	–

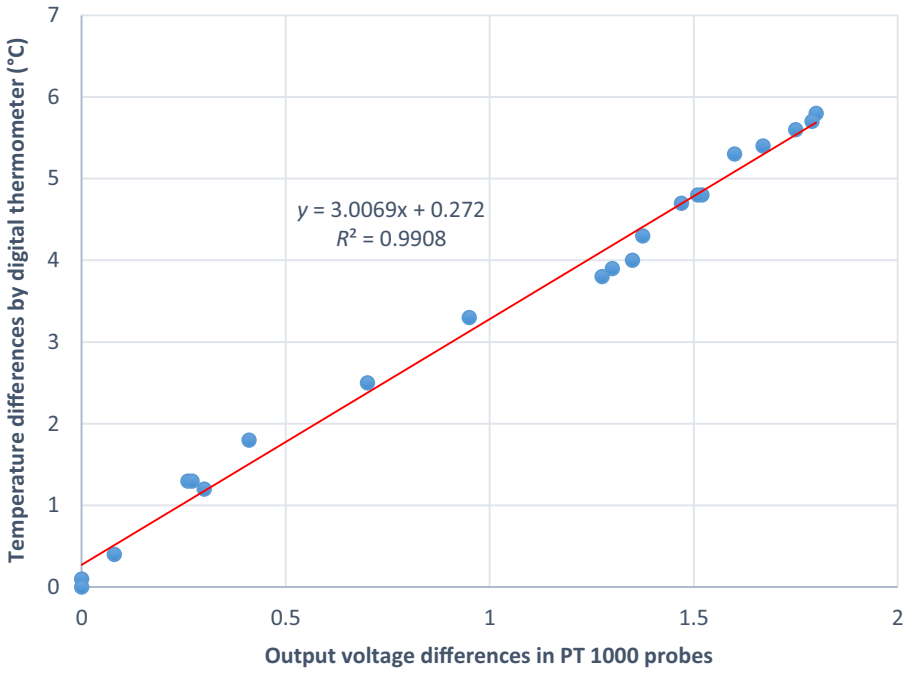

Figure 5. Relationship between the output voltage and temperatures (degC).

$$\mathrm{FWHM}\theta = 0.91\left[\sum_{z=i}^{z=n} C_{T^2}\right]^{3/5} \quad (3)$$

where z refers to each layer of the total tropospheric stratum analysed from the first layer at 2.5m to the last layer at 150m.

In this calculation, we took into account the measurements at different heights above the ground (2.5, 5, 10, 15, 20, 30, 50, 75, 100, 120 and 150m) corresponding to the height at the base of each layer. The thickness values were 2.5, 5, 5, 5, 10, 20, 25, 25, 20 and 30m. The calculation was carried out separately for each layer. This implies assuming that C_T^2 remains the same over the entire thickness of each layer. Measurements were taken at a sampling rate of 10 Hz and the average time between two successive C_T^2 estimations was 10s.

Results

First, we compared the average value of the RMS measurements (degC) with the simultaneous data for the diameter of the seeing disc FWHMθ obtained using the DIMM instruments from Calar Alto. To this end, we calculated the mean RMS value between heights of 5 and 150m for each drone flight, for which we had a minimum number of measurements of at least 8 layers (strata). These first simultaneous measurements ($n = 17$) returned an R^2 of 0.7561. In order to understand how representative this value is, it is important to bear in mind that the DIMM value reflects the turbulence for the atmosphere as a whole (Figure 8).

If we consider all the flights (including checkpoint flights), we observe that the RMS decreases with altitude. There is a good fit between the two variables (Figure 9). This preliminary evidence is in line with the results obtained by Racine (2005).

The average values for control sites for the first 150m of the PBL (also known as the Limit Layer or Ground Layer), expressed in terms of the RMS (degC) did not exceed two hundredths of a degree at any sampling point (Table 2). The lowest values were recorded at Calar Alto (0.0129 degC).

From the mean RMS (degC) value, and in accordance with expression (3), we obtained the FWHM (arcsec) (Table 2). The values represent an initial estimate of the seeing value for the lowest layer of the PBL. The most suitable values (<0.1 arcsec) occur frequently on the highest peaks.

We then analysed the results by stratum. We obtained the averaged vertical profile of the RMS at each place. This enabled us to infer the contribution made by each layer to the total seeing according to its FWHM (Figure 10). In all cases, a higher RMS value was measured in the layers closest to the ground, especially in the first 10m of height (Figure 10). At all the observatories, the differences between the RMS values became smaller at heights of 50m and greater above the ground. The difference between the layers enables us to identify the most turbulent layers and their respective heights. The results show that thermal turbulence does not make a large contribution to the seeing disc at any of the sampling points. In the area, we studied, even the highest FWHM value made a small contribution to total atmospheric seeing, in that at the observatory of La Sagra (1530m) the contribution to seeing was just 0.139 arcsec.

At all three study sites, the lowest turbulence values, <0.011 degCm^{-1}, are reached from a height of 50m upwards and are even lower from 100m. By contrast, the highest values (over 0.031 degC), and therefore the most unfavourable in an astronomical sense, were recorded in the first 5m above the ground.

Discussion and conclusions

The need to obtain high-quality astronomical images, noted by Isaac Newton as early as 1730, requires detailed studies of atmospheric turbulence, a variable with a great influence on astronomical observation.

As in other previous studies (Coulman *et al.* 1986; Bufton, 1975; Hartley *et al.*, 1981; Ulich and Davison, 1985; Ando *et al.*, 1989;

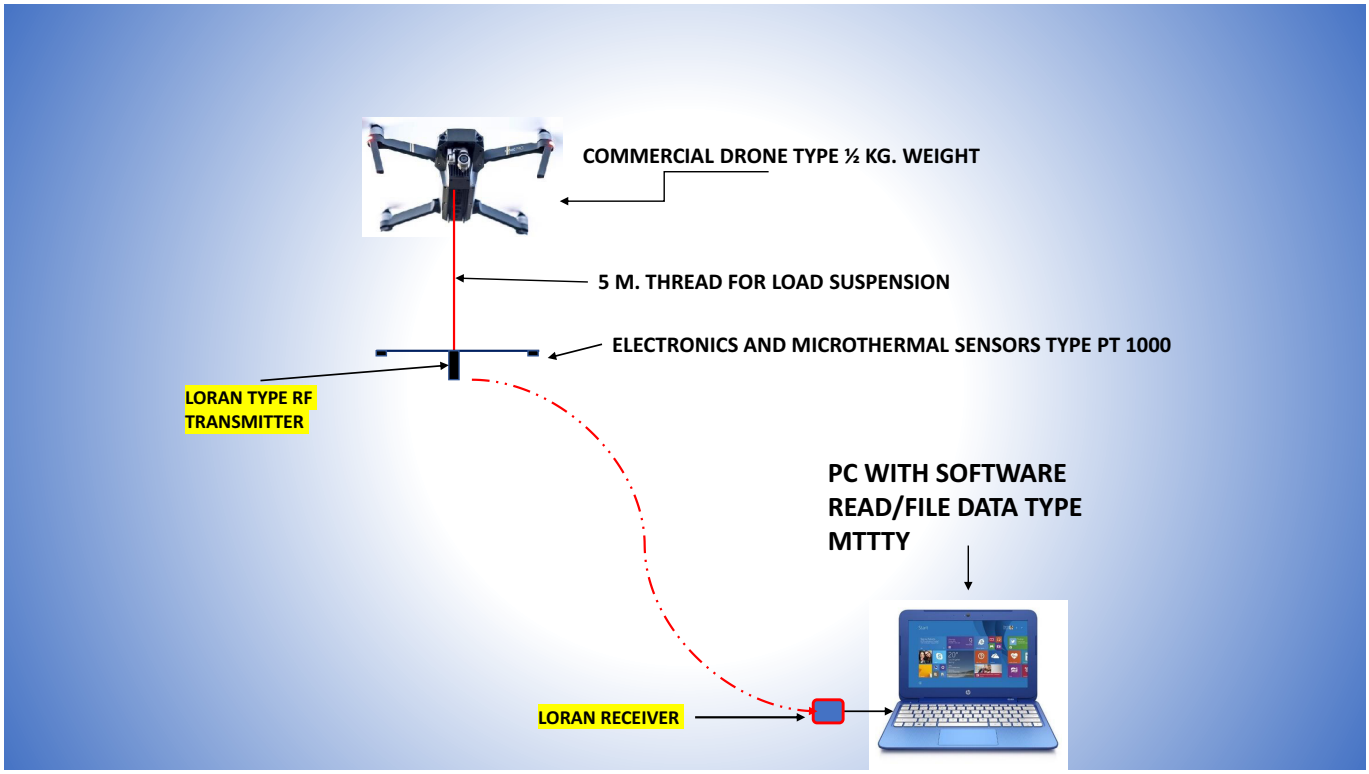

Figure 6. Drone measurement system.

Figure 7. A routine flight of the drone with microthermal sensor probe over Huetor Santillán (control site). The microthermal sensor (horizontal rod) is suspended from a 5m wire.

McHught *et al*., 2008), in this initial study, we have obtained promising results to validate the use of microthermal differential calculation in the analysis of atmospheric turbulence and as a way of assessing the quality of the astronomical images obtained at different sites (seeing). We have also tested the potential of drones for carrying out studies of this kind. Drones have the advantage that they are easy to transport to any potential location that needs to be characterised without requiring the deployment of complex, heavy equipment. Our results were tested by comparing them with those obtained by the DIMM at Calar Alto, reaching an R^2 of 0.7561. However, there are two possible limitations that may affect our results. On the one hand, the use of a digital thermometer, with a reading resolution of 0.1 degC, for the conversion of voltage outputs to temperatures. On the other hand, the small number of simultaneous measurements carried out in this temperature transformation process. However, it is also worth noting that our results returned an R^2 of 0.9908.

We also inferred the importance of the layers closest to the earth's surface (GL) in the perturbation of seeing, as a result of the higher levels of turbulence near the Earth's surface. Our results are similar to, for example, those obtained by Ando *et al*. (1989) and Vernin and Muñoz-Tuñón (1992). The contribution of the PBL to the seeing was ~0.1 arcsec in the first 150m out of the total FWHM.

Our initial approximation shows greater potential than that estimated in other parts of the Iberian Peninsula, such as Javalambre in the Sistema Ibérico mountain range (Moles *et al*., 2010) or Calar Alto (Sánchez *et al*., 2007). This would suggest, as indicated by Walker (1971), that the best-seeing values in our latitudes can be found in high, isolated mountains.

In short, if we compare our results with those obtained in other studies for other geographic areas (Racine, 2005), or with measurements made at lower altitudes at our monitoring sites, we find that in our study area, the lowest atmospheric layers nearest the Earth's surface make small contributions to the total FWHM. This suggests that erecting telescopes on top of high towers would make hardly any difference to the excellent conditions offered by sharp-pointed mountains, which in their own way already form natural towers.

In future research, we plan to continue recording microthermal differential data

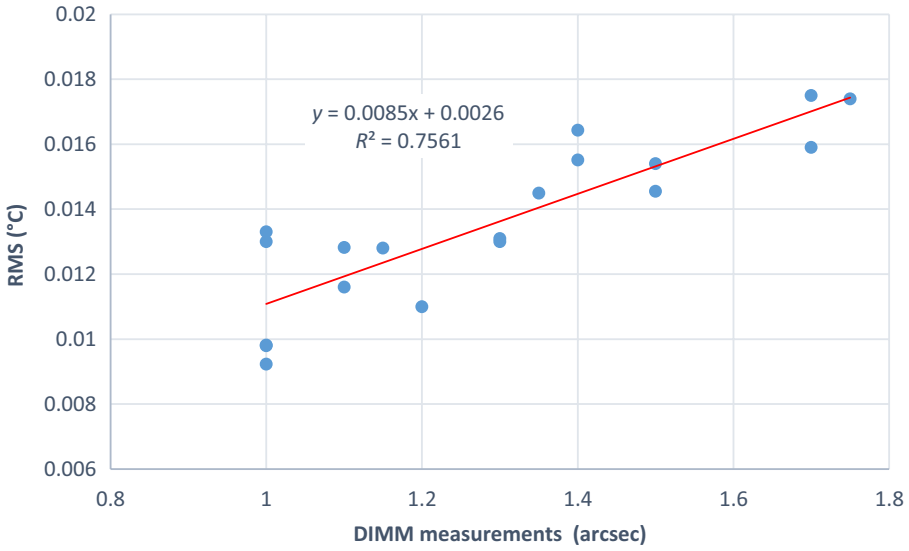

Figure 8. Relationship between the simultaneous RMS values and the DIMM value for the Calar Alto Observatory.

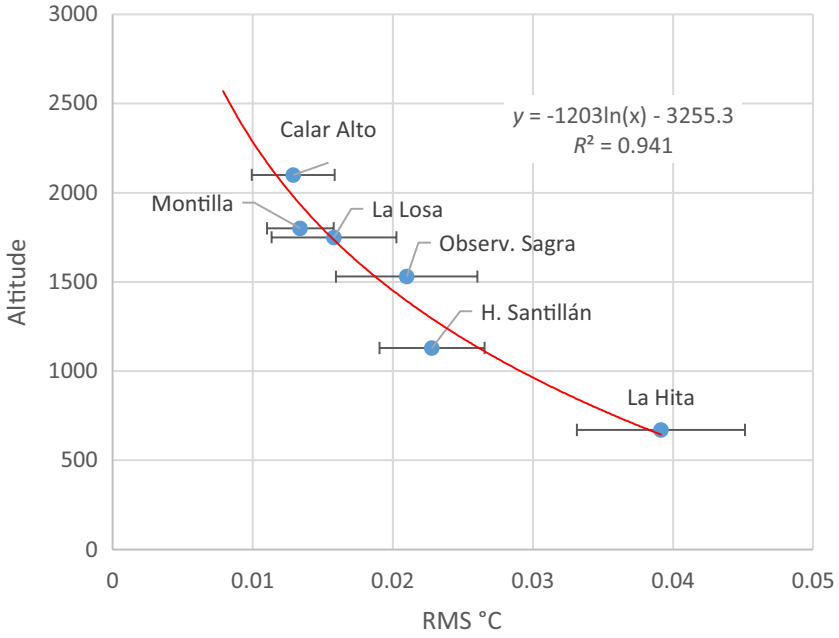

Figure 9. Relationship between altitude and average RMS with error bars (testing sites and control sites).

Table 2

RMS (degC) and FWHM (arcsec) values.

Sampling point	*Pico Montilla*	*Sagra Obsv.*	*Calar Alto*
RMS (PBL) (degC)	0.0134	0.021	0.0129
FWHM (arcsec) (PBL)	0.081	0.139	0.0977

during the night, not only with drones but also with meteorological towers.

Acknowledgements

The findings presented in this paper are partly the result of funding received by the Department of Regional Geographical Analysis and Physical Geography of the University of Granada. Funding for open access charge: Universidad de Granada / CBUA.

Author contributions

José Antonio Quesada-Moreno: Conceptualization; Data curation; Formal analysis; Investigation; Methodology; Project administration; Resources; Software; Validation; Visualization; Writing – original draft. **Emilio Martínez-Ibarra:** Funding acquisition; Investigation; Supervision; Validation; Visualization; Writing – review & editing; Methodology. **José Luis Ortiz:** Conceptualization; Project administration; Supervision; Investigation; Methodology.

Data availability statement

The data that support the findings of this study are available from the corresponding author upon reasonable request.

References

Agabi A, Aristidi E, Azouit M *et al*. 2006. First whole atmosphere nighttime seeing measurements at Dome C, Antarctica. *Publ. Astron. Soc. Pac.* **118**(840): 344–348. 10.1086/498728

Ando H, Noguchi T, Nakagiri M *et al*. 1989. Evaluation of the JNLT site. *Astrophys. Space Sci.* **160**: 183–189. doi:10.1007/BF00642769.

Barletti R, Ceppatelli G, Paterno L *et al*. 1977. Astronomical site testing with balloon borne radiosonde: results about atmospheric turbulence, solar seeing and stellar scintillation. *Astron. Astrophys.* **54**(3): 649–659.

Birkle K, Elsasser H, Neckel T *et al*. 1976. Seeing measurements in Greece, Spain, Southwest Africa, and Chile. *Astron. Astrophys.* **46**: 397–406.

Bonner CS, Ashley MCB, Cui X *et al*. 2010. Thickness of the atmospheric boundary layer above Dome A, Antarctica, during 2009. *Publ. Astron. Soc. Pac.* **122**(895): 1122–1131. doi:10.1086/656250.

Bufton JL. 1975. Radiosonde thermal sensor technique for measurement of atmospheric turbulence. Nasa Technical Note, NASA TN D-7867. https://ntrs.nasa.gov/api/citations/19750008971/downloads/19750008971.pdf.

Cavazzani S, Ortolani S, Zitelli V. 2012. Site testing at astronomical sites: evaluation of seeing using satellite-based data. *Mon. Not. R. Astron. Soc.* **419**: 3081–3091.

Cavazzani S, Rodeghiero G, Capraro I *et al*. 2014. Ground layer laser seeing meter. *Publ. Astron. Soc. Pac.* **126**(937): 312–318. doi:10.1086/676009.

Coulman CE, Andre J-C, Lacarrere P *et al*. 1986. The observation, calculation, and possible forecasting of astronomical seeing. *Publ. Astron. Soc. Pac.* **98**(601): 376–387. doi:10.1086/131769.

Dhananjay KK. 2014. Site evaluation study for the Indian National Large Solar Telescope using microthermal measurements. *Mon. Not. R. Astron. Soc.* **437**(3): 2092–2105. doi:10.1093/MNRAS/STT1985.

Egner SE, Masciadri E. 2007. A G-SCIDAR for ground-layer turbulence measurements at high vertical resolution. *Publ. Astron. Soc. Pac.* **119**(862): 1441–1448. doi:10.1086/524850.

Fossat E. 2011. Some results after 10 years of site testing at Concordia, Antarctica. arXiv:1101.3210v1. doi:10.48550/arXiv.1101.3210.

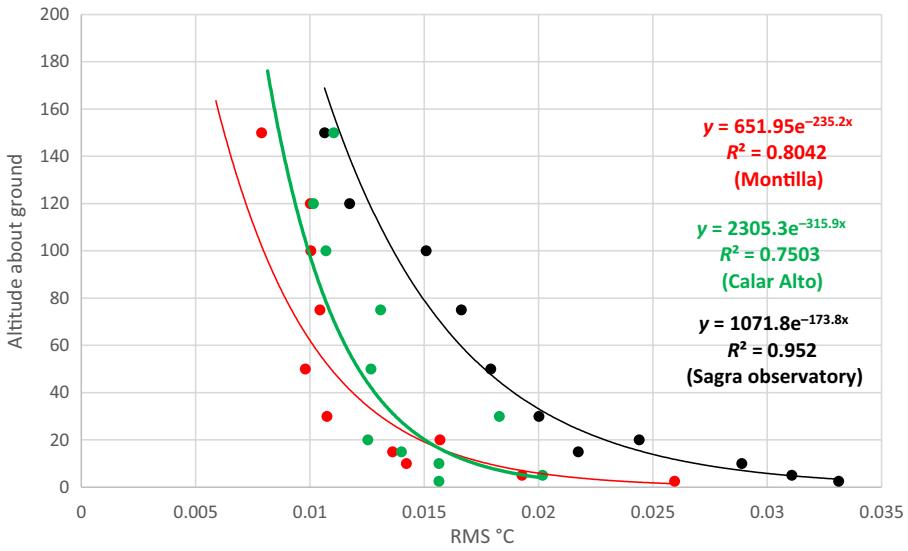

Figure 10. Vertical profiles for averaged RMS. The dots represent the mean values of the measurements in each layer, and the dashed lines represent the best-fit regression line.

Giovanelli R, **Darling J**, **Henderson C *et al***. 2001. The optical/infrared astronomical quality of high atacama sites. II. Infrared characteristics. *Publ. Astron. Soc. Pac.* **113**(785): 803–813. doi:10.1086/322136.

Hartley M, **McInnes B**, **Smith FG**. 1981. Microthermal fluctuations and their relation to seeing conditions at Roque-De La-Palma. *Q. J. R. Astron. Soc.* **22**: 272.

Lyot B. 1945. Lunar photographs taken by B. Lyot on the Pic Du Midi. *Astrophys. J.* **101**: 258.

McHught JP, **Jumper GY**, **Chun M**. 2008. Balloon thermosonde measurements over Mauna Kea and comparison with seeing measurements. *Publ. Astron. Soc. Pac.* **120**(874): 1318–1324. doi:10.1086/595871.

Moles M, **Sánchez SF**, **Lamadrid JL *et al***. 2010. Site testing of the Sierra de Javalambre: first results. *Publ. Astron. Soc. Pac.* **122**(889): 363–372. doi:10.1086/651084.

Racine R. 2005. Altitude, elevation and seeing. *Publ. Astron. Soc. Pac.* **117**(830): 401–410. doi:10.1086/429307.

Roddier F. 1981. V the effects of atmospheric turbulence in optical astronomy. *Prog. Opt.* **19**: 281–376.

Sánchez SF, **Aceituno J**, **Thiele U *et al***. 2007. The night sky at the Calar Alto Observatory. *Publ. Astron. Soc. Pac.* **119**(860): 1186–1200. doi:10.1086/522378.

Tokovinin A. 2002. From differential image motion to seeing. *Publ. Astron. Soc. Pac.* **114**(800): 1156–1166. doi:10.1086/342683.

Tokovinin A, **Baumont S**, **Vasquez J**. 2003. Statistics of turbulence profile at Cerro Tololo. *Mon. Not. R. Astron. Soc.* **340**(1): 52–58. doi:10.1046/j.1365-8711.2003.06231.x.

Ulich BL, **Davison WB**. 1985. Seeing measurements on Mount Graham. *Publ. Astron. Soc. Pac.* **97**(593): 609–615.

VanZandt TE, **Gage KS**, **Warnock JM**. 1981. An improved model for the calculation of profiles of C_N^2 and ε in the free atmosphere from background profiles of wind, temperature and humidity. In: Paper presented at Proceedings of the 20th Conference on Radar Meteorology, November 30–December 3.

VanZandt TE, **Green JL**, **Gage KS *et al***. 1978. Vertical profiles of refractivity turbulence structure constant: comparison of observations by the Sunset Radar with a new theoretical model. *Radio Sci.* **13**(5): 819–829. doi:10.1029/RS013i005p00819.

Vernin J, **Muñoz-Tuñón C**. 1992. Optical seeing at the palma observatory. I-general guidelines and preliminary results at the nordic optical telescopy. *Astron. Astrophys.* **257**(2): 811–816.

Vernin J, **Roddier F**. 1973. Experimental determination of two-dimensional spatiotemporal power spectra of stellar light scintillation: evidence for a multilayer structure of the air turbulence in the upper troposphere. *J. Opt. Soc. Am.* **63**: 270–273. doi:10.1364/JOSA.63.000270.

Walker MF. 1971. Polar star-trail observations of astronomical seeing in Arizona, Baja California, Chile y Australia. *Publ. Astron. Soc. Pac.* **83**: 401–422.

Wilson RW, **Bate J**, **Guerra JC *et al***. 2004. Development of a portable SLODAR turbulence profiler. In: Proceeding of the SPIE 5490, Advancements in Adaptive Optics, Glasgow, UK, 25 October 2004, Viewed 15 April, 2023. doi:10.1117/12.551258.

Zago L. 2010. The Effect of the Local Atmospheric Environment on Astronomical Observations. Dissertation. Swiss Federal Institute of Technology: Lausanne.

Correspondence to: E. Martínez-Ibarra
emibarra@ugr.es

doi:10.1002/wea.4551